Noncoherent Space-Time Coding for Correlated Massive MIMO Channel with Riemannian Distance

Shuangzhi Li[a,b], Xiaohang Sun[b], Yu-Hang Xiao[c], Xin Guo[a], Jiankang Zhang[d]

[a]*School of Electrical and Information Engineering, Zhengzhou University, Zhengzhou 450001, China.*
[b]*Hengdian Electronics Co., Ltd., Nanjing 210049, China*
[c]*College of Electronics and Information Engineering, Shenzhen University, Shenzhen 518060, China*
[d]*Department of Computing and Informatics, Bournemouth University, Poole BH12 5BB, U.K.*

Abstract

This paper considers a massive multiple-input multiple-output (MIMO) uplink system in correlated Rayleigh fading channels. A transmitter with two antennas needs to send data timely to a base station with a large number of antennas. We assume the channel coefficients keep constant during two consecutive time slots and change independently in the following two successive time slots. We construct a Riemannian-distance (RD) based noncoherent detector for such a system. Also, we propose a novel noncoherent parametric space-time coding method. We first attain the closed-form solutions of the optimal sub-constellation structures for fixed modulation orders with the max-min rule. Then, we determine the optimal modulation order for each sub-constellation. The analytical results show that our proposed scheme can attain a larger RD distance than the existing massive uniquely factorable constellation coding (MUFC) scheme. Further, we illustrate that our proposed coding scheme enables a low-complexity RD decoding algorithm. Simulation results show that our proposed scheme performs better than the current phase shift keying modulation scheme and MUFC scheme.

*Corresponding author:
Email Address: iexguo@zzu.edu.cn (Xin Guo)

Keywords: Massive MIMO, correlated Rayleigh fading channel, Riemannian distance, noncoherent space time coding.

1. Introduction

The massive multiple-input multiple-output (MIMO) technique has attracted significant attention from the industry and academics due to its high spectral and energy efficiency [1]. It is widely considered one of the fundamental technologies for fifth-generation (5G) wireless communications. Especially, massive MIMO is regarded as a promising contributor to ultra-reliable low-latency communication (URLLC) [2], which is a crucial feature brought by 5G; URLLC will be used in mission-critical communications, like reliable remote robots. For critical use cases, it is anticipated to achieve a probability of error down to 10^{-5} to 10^{-9} and an air interface latency down to 1ms in a single transmission with tens of bytes long [3]. Due to the strict constraint on latency and reliability, it requires a reevaluation of the current physical layer design approaches. Among them, the short data packet transmission is considered to be the main feature that needs to be tailored to the physical layer for URLLC [4]. With reliable and quasi-deterministic links, massive MIMO systems are expected to be the main enabler for the transmission of the short data packet. Nevertheless, the benefits of massive MIMO are conditioned on the acquisition of the instantaneous channel state information (CSI), particularly at the massive base station (BS) [2]. For coherent training-based signaling schemes, the transmitter requires to transmit pilot sequences to the BS periodically [1, 5]. The BS can estimate the instantaneous CSI with simple linear estimators, like the least square and linear minimum mean square error method [5]. Then, the BS can decode the following data symbols by regarding the estimated CSI as the accurate CSI. With such a scheme, the massive MIMO can be exploited for URLLC under low-mobility conditions [2]. However, the number of coherent time slots in high mobility conditions is limited. There will be not enough coherent time slots for the transmission of data symbols. Moreover, the usage of pilot sequences may introduce a certain latency and training overhead [6].

As an alternate method, noncoherent transmissions have regained the attention of researchers, in which neither the transmitter nor the receiver requires instantaneous prior knowledge of CSI [7]. Over the last two decades, considerable efforts have been dedicated to noncoherent coding schemes in typical MIMO systems with fewer antennas at both the transmitter and receiver ends [8, 9, 10, 11]. These work mainly focused on unitary space-time code designs since unitary constellations are optimal when the signal-to-noise ratio (SNR) is high or the number of coherent time slots is large. With the advent of massive MIMO technology, some works have initially reconsidered the noncoherent constellation design criteria [12, 13, 14, 15, 16, 17, 18]. In particular, the favorable propagation condition of a large number of antennas is widely used in signal optimization criteria and constellation design [12, 13, 14, 15, 16, 17, 18]. In [12, 13, 18], noncoherent space-time modulations are proposed for multi-users by using PSK modulations methods. In [15, 16, 17], one-slot symbol-by-symbol detection with pulse amplitude modulation (PAM) constellations is used to convey information bits. Unfortunately, the symbol-by-symbol detection scheme cannot leverage the transmitted signal's phase to convey information, resulting in low spectral efficiency. Motivated by this, in [13], based on the Riemannian distance (RD) criterion, a massive uniquely factorable constellation (MUFC) is exploited to convey information bits during two consecutive coherent time slots in a massive single-input multiple-output (SIMO) system [13, 14], which conveys information bits on multidimensional parameter spaces and has shown superior performance to the PAM constellations, especially in the low SNR scenario and large antenna region. The proposed MUFC can achieve the maximum RD distance under the power constraint and transmission rate based on the max-min rule. However, whether there exist benefits for the MUFC scheme when using multiple antennas at the transmitter has not yet been explored. Also, we note that the aforementioned noncoherent coding work focused on independent and identically distributed (i.i.d.) Rayleigh fading channels and a few works involved correlated Rayleigh fading channels.

In [17], a modified PAM constellation is proposed for a massive SIMO system, which shows that the correlation factor can be exploited to improve the considered system's error performance with an emphasis on the design of a novel noncoherent detector and space-time constellation design. In this paper, we consider a massive MIMO system under correlated Rayleigh fading channels, in which a transmitter with two antennas sends data timely to a BS with many antennas. Also, we assume the correlation matrix can keep constant in multiple time slots. At the same time, the instantaneous CSI remains unchanged for a coherence time of two symbols, after which they change into new independent values that keep fixed for the following two consecutive time slots. Since the orthogonal pilot overhead scales linearly with the number of transmitting antennas, there will not be enough time slots for data symbols with a coherent transmission scheme [19]. For such a system, we focus on designing a noncoherent detector and constructing the noncoherent space-time constellations for a massive MIMO system under correlated Rayleigh fading channels. The main contributions of our work can be summarized as follows:

1. We propose a modified RD-based detector for a massive MIMO uplink system under correlated Rayleigh fading channels.
2. A novel noncoherent parametric space-time coding scheme is proposed based on the max-min rule for RD-based detector. The optimal design for the proposed detector is theoretically derived and has a larger RD distance than the existing MUFC coding scheme proposed in [14].
3. A low complexity decoding algorithm is derived for the proposed coding scheme to decrease the signal processing delay further.

Notations: Matrices are denoted by uppercase boldface characters (e.g., $\mathbf{A}$), while column vectors are denoted by lowercase boldface characters (e.g., $\mathbf{b}$). $(\cdot)^*$, $(\cdot)^T$, $(\cdot)^H$, and $|\cdot|$ denote the conjugate, transpose, conjugate transpose, and absolute value operation, respectively. $\mathrm{tr}(\cdot)$ and $\angle(\cdot)$ denote the trace and angle operation, respectively. $\mathbb{Z}$ denotes the ring of integers; $\mathbb{C}$ denotes the field of complex number. The Euclidean norm is denoted as $||\cdot||$. $\mathbf{I}_K$ denotes the $K \times K$ identity matrix. $\Re\{\cdot\}$ denotes the real part of a complex number. $j \triangleq \sqrt{-1}$. $|\mathcal{S}|$ denotes the cardinality of the constellation $\mathcal{S}$. The operator $\mathrm{diag}\{\mathbf{a}\}$ forms a diagonal matrix out of its vector argument.

2. System Model

In this paper, we consider a massive MIMO uplink system, in which a transmitter equipped with two antennas timely transmits data to a BS having M antennas[1]. We denote the channel between the transmitter and BS is $\mathbf{G} \in \mathbb{C}^{M\times 2}$. In this system, we use the IEEE 802.11n MIMO channel model [20, 21] represents the diffuse multipath component by a stochastic process including properties between antenna signals [22], i.e.,

$$\mathbf{G} = (\mathbf{R}_{Rx})^{\frac{1}{2}}\mathbf{H}((\mathbf{R}_{Tx})^{\frac{1}{2}})^T, \tag{1}$$

[1]To extend our proposed scheme to multiple users, one possible way is to resort to the time-division multiple access scheme, i.e., allocating separate orthogonal time slots to each user.

where $\mathbf{R}_{Rx} \in \mathbb{C}^{M\times M}$ and $\mathbf{R}_{Tx} \in \mathbb{C}^{2\times 2}$ are spatial correlation matrices for the receiver antennas and transmitter antennas. $\mathbf{H}$ is a matrix of independent zero mean, unit variance, complex Gaussian random variables. Since the transmitter only has two antennas, the antenna can always be spaced sufficiently apart so that they become uncorrelated. Therefore, we assume $\mathbf{R}_{Tx} = \mathbf{I}_2$. For the sake of notation simplicity, we denote $\mathbf{G} = \mathbf{R}^{\frac{1}{2}}\mathbf{H}$ with $\mathbf{R} \in \mathbb{C}^{M\times M}$ and $[\mathbf{H}]_{ij} \in \mathcal{CN}(0,1)$. We consider a block-fading communication scenario, in which the channel keeps constant during two time slots, after which they change into independent values.

Also, we assume $\mathbf{R}$ is previously known at the BS, and its eigenvalue decomposition (EVD) can be expressed as $\mathbf{R} = \mathbf{U}_R\mathbf{\Sigma}\mathbf{U}_R^H$, in which $\mathbf{U}_R \in \mathbb{C}^{M\times M}$ is a unitary matrix with $\mathbf{U}_R^H\mathbf{U}_R = \mathbf{U}_R\mathbf{U}_R^H = \mathbf{I}_M$. $\mathbf{\Sigma} = \text{diag}\{\boldsymbol{\lambda}\} = \text{diag}\{\lambda_1, \cdots, \lambda_M\}$, $\lambda_1 \geq \cdots \geq \lambda_M \geq 0$ is a real diagonal matrix consisting of all the eigenvalues. $\mathbf{R}$ can keep constant during multiple time slots because it is far less frequently varying than the instantaneous CSI matrix $\mathbf{H}$.

At the transmitter end, a space-time coding matrix $\mathbf{S} \in \mathbb{C}^{2\times 2}$ encodes message with the power constraint $\mathbb{E}\{\text{tr}\{\mathbf{S}^H\mathbf{S}\}\} = 1$. Then, the received signal matrix $\mathbf{Y} \in \mathbb{C}^{M\times 2}$ at BS can be represented as

$$\mathbf{Y} = \mathbf{R}^{\frac{1}{2}}\mathbf{H}\mathbf{S} + \mathbf{N}, \tag{2}$$

where $\mathbf{N} \in \mathbb{C}^{M\times 2}$ is the noise matrix, the elements following i.i.d. complex Gaussian distribution, i.e., $[\mathbf{N}]_{ij} \in \mathcal{CN}(0, \sigma_n^2)$. For such a system, we consider a noncoherent transmission scheme, focus on recovering the signal matrix $\mathbf{S}$ from the statistical information of $\mathbf{Y}$ without the instantaneous CSI $\mathbf{H}$. First, we take a pre-processing of $\mathbf{Y}$ by multiplying $\mathbf{\Sigma}^{-\frac{1}{2}}\mathbf{U}_R^H$. For the sake of simplicity, we denote $\tilde{\mathbf{Y}} = \mathbf{\Sigma}^{-\frac{1}{2}}\mathbf{U}_R^H\mathbf{Y}$. Then, we can rebuild (2) as

$$\tilde{\mathbf{Y}} = \tilde{\mathbf{H}}\mathbf{S} + \tilde{\mathbf{N}}, \tag{3}$$

where $\tilde{\mathbf{H}} = \mathbf{U}_R^H\mathbf{H}$ and $\tilde{\mathbf{N}} = \mathbf{\Sigma}^{-\frac{1}{2}}\mathbf{U}_R^H\mathbf{N}$. With (3), we can arrive at Proposition 1.

Proposition 1. *With M increasing, in correlated Rayleigh fading massive MIMO uplink network, we can attain*

$$\arg\min_{\mathbf{A}} \mathbb{E}\Big\{\|\frac{\tilde{\mathbf{Y}}^H\tilde{\mathbf{Y}}}{M} - \mathbf{A}\|_F^2\Big\} = \mathbf{S}^H\mathbf{S} + \frac{tr\{\mathbf{\Sigma}^{-1}\}}{M}\sigma_n^2\mathbf{I}_2. \tag{4}$$

The proof of Proposition 1 is provided in Appendix A.

Besides, we can use an RD-based detector for (3) based on the least square (LS) criterion [13, 14]:

$$\begin{aligned}\hat{\mathbf{S}} &= \arg\min_{\mathbf{S}\in\mathcal{S}} \frac{1}{M}\|\tilde{\mathbf{Y}} - \tilde{\mathbf{H}}\mathbf{S}\|_F^2 \\ &= \arg\min_{\mathbf{S}\in\mathcal{S}} \operatorname{tr}\Big\{\frac{\tilde{\mathbf{Y}}^H\tilde{\mathbf{Y}}}{M}\Big\} + \operatorname{tr}\{\mathbf{S}^H\mathbf{S}\} - 2\operatorname{tr}\{(\frac{\tilde{\mathbf{Y}}^H\tilde{\mathbf{Y}}}{M}\mathbf{S}^H\mathbf{S})^{\frac{1}{2}}\}. \end{aligned} \tag{5}$$

By jointly considering (4) and (5), a noncoherent RD-based detector for the massive MIMO uplink communication system under correlated Rayleigh fading channel can be finally formulated as

$$\begin{aligned}\hat{\mathbf{S}} = \arg\min_{\mathbf{S}\in\mathcal{S}} \operatorname{tr}\Big\{\frac{\tilde{\mathbf{Y}}^H\tilde{\mathbf{Y}}}{M} - \frac{\operatorname{tr}\{\mathbf{\Sigma}^{-1}\}}{M}\sigma_n^2\mathbf{I}_2\Big\} + \operatorname{tr}\{\mathbf{S}^H\mathbf{S}\} \\ - 2\operatorname{tr}\Big\{\Big[(\frac{\tilde{\mathbf{Y}}^H\tilde{\mathbf{Y}}}{M} - \frac{\operatorname{tr}\{\mathbf{\Sigma}^{-1}\}}{M}\sigma_n^2\mathbf{I}_2)\mathbf{S}^H\mathbf{S}\Big]^{\frac{1}{2}}\Big\}, \end{aligned} \tag{6}$$

where $\mathcal{S}$ is the space-time constellation set for $\mathbf{S}$. Based on the max-min rule, the optimization framework with RD criterion for $\mathcal{S}$ can be built as

$$\begin{aligned}\hat{\mathcal{S}} = \arg\max_{\mathcal{S}} &\min_{\forall \mathbf{S}_i,\mathbf{S}_j\in\mathcal{S},\mathbf{S}_i\neq\mathbf{S}_j} \operatorname{tr}\{\mathbf{S}_i^H\mathbf{S}_i\} + \operatorname{tr}\{\mathbf{S}_j^H\mathbf{S}_j\} - 2\operatorname{tr}\{(\mathbf{S}_i^H\mathbf{S}_i\mathbf{S}_j^H\mathbf{S}_j)^{\frac{1}{2}}\} \\ s.t. \quad & \mathbb{E}\{\operatorname{tr}\{\mathbf{S}_i^H\mathbf{S}_i\}\} = 1, \\ & \mathbb{E}\{\operatorname{tr}\{\mathbf{S}_j^H\mathbf{S}_j\}\} = 1. \end{aligned} \tag{7}$$

where $\mathbf{S}_i$ and $\mathbf{S}_j$ are any two distinct entries in $\mathcal{S}$.

3. Parametric Space-time Coding with Alamouti Code structure

This section is dedicated to constructing $\mathcal{S}$ for the considered system and finding the optimal solution to the problem given in (7). Our main idea is to determine the objective function in (7) explicitly. Then, based on the max-min rule, we can first determine the optimal constellation structure for the fixed modulation order scheme. Finally, we can determine the optimal modulation orders to maximize the objection functions minimum value further.

3.1. Parametric Space-time Coding Scheme

The matrix $\mathbf{S}$ is constructed by an Alamouti code matrix $\mathbf{U}$ with $\mathbf{U}^H\mathbf{U} = \mathbf{U}\mathbf{U}^H = \mathbf{I}_2$ and a power allocation matrix $\mathbf{P}$ with $\mathbf{P} = \mathrm{diag}([p_1, p_2]), p_1, p_2 \geq 0$ satisfying $\mathbf{S} = \mathbf{P}^{\frac{1}{2}}\mathbf{U}$. First, $\mathbf{U}$ can be parameterized as

$$\mathbf{U} = \begin{pmatrix} e^{j\phi_1}\cos(\theta) & e^{j\phi_2}\sin(\theta) \\ -e^{-j\phi_2}\sin(\theta) & e^{-j\phi_1}\cos(\theta) \end{pmatrix}, \tag{8}$$

where $0 \leq \phi_1, \phi_2 < 2\pi$, and $0 \leq \theta \leq \frac{\pi}{2}$. In (8), $\cos(\theta)$ and $\sin(\theta)$ represent the amplitude information of transmitted symbols in $\mathbf{U}$. Further, we can rewrite $\mathbf{U}$ as

$$\mathbf{U} = \begin{pmatrix} e^{j\phi_1} & 0 \\ 0 & e^{-j\phi_1} \end{pmatrix} \begin{pmatrix} \cos(\theta) & e^{j\phi}\sin(\theta) \\ -e^{-j\phi}\sin(\theta) & \cos(\theta) \end{pmatrix}, \tag{9}$$

where $\phi = \phi_2 - \phi_1$ with $0 \leq \phi < 2\pi$. Then, $\mathbf{S}$ can be written as:

$$\mathbf{S} = \begin{pmatrix} \sqrt{p_1} & 0 \\ 0 & \sqrt{p_2} \end{pmatrix} \begin{pmatrix} e^{j\phi_1} & 0 \\ 0 & e^{-j\phi_1} \end{pmatrix} \begin{pmatrix} \cos(\theta) & e^{j\phi}\sin(\theta) \\ -e^{-j\phi}\sin(\theta) & \cos(\theta) \end{pmatrix}. \tag{10}$$

To ensure the unique identification of $\mathbf{S}$ with the RD receiver, $\mathbf{S}^H\mathbf{S}$ should be uniquely identified. Therefore, $\mathrm{diag}\{[e^{j\phi_1}, e^{-j\phi_1}]\}$ can be ignored. Let $a \triangleq \sqrt{p_1}$ and $b \triangleq \sqrt{p_2}$, $\mathbf{S}$ can be equivalently transformed into

$$\mathbf{S} = \begin{pmatrix} a & 0 \\ 0 & b \end{pmatrix} \begin{pmatrix} \cos(\theta) & e^{j\phi}\sin(\theta) \\ -e^{-j\phi}\sin(\theta) & \cos(\theta) \end{pmatrix}, \tag{11}$$

where $a \geq 0$ and $b \geq 0$ under the power constraint $\mathbb{E}\{\mathrm{tr}(\mathbf{S}^H\mathbf{S})\} = \mathbb{E}\{a^2\} + \mathbb{E}\{b^2\} = 1$, $0 \leq \theta \leq \frac{\pi}{2}$, $0 \leq \phi < 2\pi$.

Note that when $b = 0$, the proposed scheme degrades to the MUFC scheme proposed in the massive SIMO uplink system [14]. In this paper, we will investigate whether the increased number of transmitter antennas can improve the coding gain of MUFC.

Let us denote $\mathbf{S}_i \triangleq \begin{pmatrix} a_i & 0 \\ 0 & b_i \end{pmatrix} \begin{pmatrix} \cos\theta_i & e^{j\phi_i}\sin\theta_i \\ -e^{-j\phi_i}\sin\theta_i & \cos\theta_i \end{pmatrix}$ and $\mathbf{S}_j \triangleq \begin{pmatrix} a_j & 0 \\ 0 & b_j \end{pmatrix} \begin{pmatrix} \cos\theta_j & e^{j\phi_j}\sin\theta_j \\ -e^{-j\phi_j}\sin\theta_j & \cos\theta_j \end{pmatrix}$. Then, for the objective function in (7), we can attain $\mathrm{tr}\{\mathbf{S}_i^H\mathbf{S}_i\} = a_i^2 + b_i^2$ and $\mathrm{tr}\{\mathbf{S}_j^H\mathbf{S}_j\} = a_j^2 + b_j^2$. Besides, we have $\mathrm{tr}\{(\mathbf{S}_i^H\mathbf{S}_i\mathbf{S}_j^H\mathbf{S}_j)^{\frac{1}{2}}\} = \mathrm{tr}\{(\mathbf{S}_j\mathbf{S}_i^H\mathbf{S}_i\mathbf{S}_j^H)^{\frac{1}{2}}\}$. Since $\mathbf{S}_j\mathbf{S}_i^H\mathbf{S}_i\mathbf{S}_j^H$ is a two-by-two semi-positive matrix, we can achieve

$$\begin{aligned}\mathrm{tr}\{(\mathbf{S}_j\mathbf{S}_i^H\mathbf{S}_i\mathbf{S}_j^H)^{\frac{1}{2}}\} &= \sqrt{\mathrm{tr}\{\mathbf{S}_j\mathbf{S}_i^H\mathbf{S}_i\mathbf{S}_j^H\} + 2(\det\{\mathbf{S}_j\mathbf{S}_i^H\mathbf{S}_i\mathbf{S}_j^H\})^{\frac{1}{2}}} \\ &= \sqrt{(a_ib_j + b_ia_j)^2 + (a_i^2 - b_i^2)(a_j^2 - b_j^2)\Xi(\theta_i, \theta_j, \phi_i, \phi_j)},\end{aligned} \tag{12}$$

where

$$\Xi(\theta_i, \theta_j, \phi_i, \phi_j) = \cos^2\theta_i\cos^2\theta_j + \sin^2\theta_i\sin^2\theta_j + 2\sin\theta_i\cos\theta_i\sin\theta_j\cos\theta_j\cos(\phi_i - \phi_j)$$

.

Also, we attain

$$\det\{\mathbf{S}_j\mathbf{S}_i^H\mathbf{S}_i\mathbf{S}_j^H\} = a_i^2b_i^2a_j^2b_j^2. \tag{13}$$

By combing (12) and (13), the objective function in (7) can be expressed explicitly,

$$\begin{aligned}&\mathrm{tr}\{\mathbf{S}_i^H\mathbf{S}_i\} + \mathrm{tr}\{\mathbf{S}_j^H\mathbf{S}_j\} - 2\mathrm{tr}\{(\mathbf{S}_i^H\mathbf{S}_i\mathbf{S}_j^H\mathbf{S}_j)^{\frac{1}{2}}\} \\ &= a_i^2 + b_i^2 + a_j^2 + b_j^2 - 2\sqrt{(a_ib_j + b_ia_j)^2 + (a_i^2 - b_i^2)(a_j^2 - b_j^2)\Xi(\theta_i, \theta_j, \phi_i, \phi_j)}.\end{aligned} \tag{14}$$

Remark: We observe that when $a_i = b_i$ and $a_j = b_j$, the value of (14) equals zero. Also, when $a_i = b_j$, $b_i = a_j$, $\theta_i = \frac{\pi}{2} - \theta_j$ and $\phi_i = \pi - \phi_j$, the value of (14) degrades to zero. In other words, when $a_i > b_i$, there always exists a scenario for $a_j < b_j$, that has zero RD with $a_i > b_i$. In such cases, the receiver can not distinguish $\mathbf{S}_i$ and $\mathbf{S}_j$. Given this, we further assume that $a > b$ in (11) to ensure reliable transmission. Then, by using the polar coordinate, we further parameterize $a \triangleq \sqrt{p}\cos(\tau)$ and $b \triangleq \sqrt{p}\sin(\tau)$ with $0 \le \tau < \frac{\pi}{4}$ and $p > 0$.

Based on the above discussions, we can parameterize our proposed space-time constellation $\mathcal{S}$ as

$$\mathcal{S} = \left\{\mathbf{S} \in \mathcal{S} \middle| \mathbf{S} = \sqrt{p}\begin{pmatrix}\cos(\tau) & 0 \\ 0 & \sin(\tau)\end{pmatrix}\begin{pmatrix}\cos(\theta) & e^{j\phi}\sin(\theta) \\ -e^{-j\phi}\sin(\theta) & \cos(\theta)\end{pmatrix}\right\}, \tag{15}$$

where $p \ge 0$, $0 \le \tau < \frac{\pi}{4}$, $0 \le \theta \le \frac{\pi}{2}$, and $0 \le \phi < 2\pi$. Our aim is to determine four sub-constellations $\mathcal{P}$, $\mathcal{T}$, Θ, and Φ, correspondingly, where $\sqrt{p} \in \mathcal{P}$, $\tau \in \mathcal{T}$, $\theta \in \Theta$ and $e^{j\phi} \in \Phi$ that satisfy the constraints in (7).

3.2. Closed-form Solution of Optimal $\mathcal{S}$

With the parametric structure of $\mathcal{S}$ in (15), (14) can be transformed into (16):

$$\begin{aligned} &\mathrm{tr}\{\mathbf{S}_i^H\mathbf{S}_i\} + \mathrm{tr}\{\mathbf{S}_j^H\mathbf{S}_j\} - 2\mathrm{tr}\{(\mathbf{S}_i^H\mathbf{S}_i\mathbf{S}_j^H\mathbf{S}_j)^{\frac{1}{2}}\} \\ &= p_i + p_j - 2p_i^{1/2}p_j^{1/2}\sqrt{\sin^2(\tau_i+\tau_j) + \cos(2\tau_i)\cos(2\tau_j)\Xi(\theta_i,\theta_j,\phi_i,\phi_j)}. \end{aligned} \quad (16)$$

We assume the $\sqrt{p}$, τ, θ, and $e^{j\phi}$ are independently chosen from $\mathcal{P}$ with $|\mathcal{P}| = 2^{k_p}$, $\mathcal{T}$ with $|\mathcal{T}| = 2^{k_\tau}$, Θ with $|\Theta| = 2^{k_\theta}$ and Φ with $|\Phi| = 2^{k_\phi}$, where k_p, k_τ, k_θ, and k_ϕ are the corresponding modulation orders. To achieve the optimal $\mathcal{S}$, we can instead determine the optimal $\hat{\mathcal{P}}$, $\hat{\mathcal{T}}$, $\hat{\Theta}$, and $\hat{\Phi}$. The main solution is here: first, we will determine the optimal structure of $\hat{\mathcal{P}}$, $\hat{\mathcal{T}}$, $\hat{\Theta}$, and $\hat{\Phi}$ for each scenario and the optimal solution for the achieved minimum RD. Finally, we will determine the optimal modulation orders of the four sub-constellations. For the first step, we can attain Proposition 2.

Proposition 2. *For fixed k_p, k_τ, k_θ, and k_ϕ, the optimal $\mathcal{P}$ follows an arithmetic sequence with $\hat{\mathcal{P}} = \{\sqrt{p_0}, \sqrt{p_0} + \Delta p, \cdots, \sqrt{p_0} + (2^{k_p} - 1)\Delta p\}$ with $|\hat{\mathcal{P}}| = 2^{k_p}$ and $p_0 \geq 0$; the optimal $\mathcal{T}$ is also an arithmetic sequence $\hat{\mathcal{T}} = \{0, \Delta\tau, \cdots, \tau_c\}$ with $\Delta\tau = \frac{\tau_c}{2^{k_\tau}-1}$ and $|\hat{\mathcal{T}}| = 2^{k_\tau}$, $0 \leq \tau_c \leq \frac{\pi}{4}$; the optimal Θ follows an arithmetic sequence with $\hat{\Theta} = \{\theta_0, \theta_0 + \Delta\theta, \cdots, \frac{\pi}{2} - \theta_0\}$, $\Delta\theta = \frac{\pi/2-2\theta_0}{2^{k_\theta}-1}$, and $|\hat{\Theta}| = 2^{k_\theta}$ $(0 \leq \theta_0 \leq \frac{\pi}{2})$; the optimal Φ satisfies $\hat{\Phi} = 2^{k_\phi}$-PSK. Denote the achieved maximal RD for each set of $(k_p, k_\tau, k_\theta, k_\phi)$ is*

$$\begin{aligned} &d_{R_1}(k_p, k_\tau, k_\theta, k_\phi) \triangleq d_{R_1}(p_i, p_j, \tau_i, \tau_j, \theta_i, \theta_j, \phi_i, \phi_j) \\ &\triangleq \max \min_{\forall \mathbf{S}_i, \mathbf{S}_j \in \mathcal{S}, \mathbf{S}_i \neq \mathbf{S}_j} \sqrt{\mathrm{tr}\{\mathbf{S}_i^H\mathbf{S}_i\} + \mathrm{tr}\{\mathbf{S}_j^H\mathbf{S}_j\} - 2\,\mathrm{tr}\{(\mathbf{S}_i^H\mathbf{S}_i\mathbf{S}_j^H\mathbf{S}_j)^{\frac{1}{2}}\}}. \end{aligned}$$

The key parameters p_0, Δp, τ_c, θ_0, and $d(k_p, k_\tau, k_\theta, k_\phi)$ with optimal sub-constellations can be determined with closed-form solutions as[2]*:*

1. *when $k_\tau = 0$, $k_p \neq 0$, $k_\theta \neq 0$, and $k_\phi \neq 0$: $\tau_c = 0$; θ_0 is the solution to the equation $\sin(2\theta_0)\sin(\frac{\pi}{2^{k_\phi}}) = \sin(\frac{\pi/2-2\theta_0}{2^{k_\theta}-1})$, $p_0 = \frac{3}{\Omega_1}$ with*

$$\Omega_1 \triangleq 3 + 6(2^{k_p} - 1)\sin(\frac{\pi/4 - \theta_0}{2^{k_\theta} - 1}) + 2(2^{k_p} - 1)(2^{k_p+1} - 1)\sin^2(\frac{\pi/4 - \theta_0}{2^{k_\theta} - 1}),$$

[2] There exist 15 scenarios for possible combinations $(k_p, k_\tau, k_\theta, k_\phi)$ since at least one parameter is a positive integer.

and $\Delta p = 2\sin(\frac{\pi/4-\theta_0}{2^{k_\theta}-1})\sqrt{\frac{3}{\Omega_1}}$. *In such a case,* $d_{R_1}(k_p, k_\tau, k_\theta, k_\phi) = \Delta p$.

2. *when* $k_\tau = 0$, $k_p = 0$, $k_\theta \neq 0$, *and* $k_\phi \neq 0$: $\tau_c = 0$; $p_0 = 1$ *and* $\Delta p = 0$; θ_0 *is the solution to* $\sin(2\theta_0)\sin(\frac{\pi}{2^{k_\phi}}) = \sin(\frac{\pi/2-2\theta_0}{2^{k_\theta}-1})$; *In such a case,* $d_{R_1}(k_p, k_\tau, k_\theta, k_\phi) = 2\sin(\frac{\pi/4-\theta_0}{2^{k_\theta}-1})$.
3. *when* $k_\tau = 0$, $k_p \neq 0$, $k_\theta = 0$, *and* $k_\phi \neq 0$: $\tau_c = 0$; $\theta_0 = \frac{\pi}{4}$; $p_0 = \frac{3}{\Omega_2}$ *with*

$$\Omega_2 \triangleq 3 + 6(2^{k_p} - 1)\sin(\frac{\pi}{2^{k_\phi+1}}) + 2(2^{k_p} - 1)(2^{k_p+1} - 1)\sin^2(\frac{\pi}{2^{k_\phi+1}}),$$

and $\Delta p = 2\sqrt{\frac{3}{\Omega_2}}\sin(\frac{\pi}{2^{k_\phi+1}})$. *In such a case,* $d_{R_1}(k_p, k_\tau, k_\theta, k_\phi) = \Delta p$.

4. *when* $k_\tau = 0$, $k_p \neq 0$, $k_\theta \neq 0$, *and* $k_\phi = 0$: $\tau_c = 0$; $\theta_0 = 0$; $p_0 = \frac{3}{\Omega_3}$ *with*

$$\Omega_3 \triangleq 3 + 6(2^{k_p} - 1)\sin(\frac{\pi}{2^{k_\theta+2}}) + 2(2^{k_p} - 1)(2^{k_p+1} - 1)\sin^2(\frac{\pi}{2^{k_\theta+2}}),$$

and $\Delta p = 2\sin(\frac{\pi}{2^{k_\theta+2}})\sqrt{\frac{3}{\Omega_3}}$. *In such as case,* $d_{R_1}(k_p, k_\tau, k_\theta, k_\phi) = \Delta p$.

5. *when* $k_\tau = 0$, $k_p = 0$, $k_\theta = 0$, *and* $k_\phi \neq 0$: $\tau_c = 0$; $p_0 = 1$ *and* $\Delta p = 0$; $\theta_0 = \frac{\pi}{4}$; *In such a case,* $d_{R_1}(k_p, k_\tau, k_\theta, k_\phi) = 2\sin(\frac{\pi}{2^{k_\phi+1}})$.
6. *when* $k_\tau = 0$, $k_p = 0$, $k_\theta \neq 0$, *and* $k_\phi = 0$: $\tau_c = 0$; $p_0 = 1$ *and* $\Delta p = 0$; $\theta_0 = 0$; *In such a case,* $d_{R_1}(k_p, k_\tau, k_\theta, k_\phi) = 2\sin(\frac{\pi}{4(2^{k_\theta}-1)})$.
7. *when* $k_\tau = 0$, $k_p \neq 0$, $k_\theta = 0$, *and* $k_\phi = 0$: $\tau_c = 0$; $\theta_0 = \frac{\pi}{4}$; $p_0 = 0$ *and* $\Delta p = \sqrt{\frac{6}{(2^{k_p}-1)(2^{k_p+1}-1)}}$. *In such a case,* $d_{R_1}(k_p, k_\tau, k_\theta, k_\phi) = \Delta p$.
8. *when* $k_\tau \neq 0$, $k_p \neq 0$, $k_\theta \neq 0$, *and* $k_\phi \neq 0$: θ_0 *is the solution to* $\sin(2\theta_0)\sin(\frac{\pi}{2^{k_\phi}}) = \sin(\frac{\pi/2-2\theta_0}{2^{k_\theta}-1})$; $\tau_c \in [0, \frac{\pi}{4})$ *is the solution to the equation* $\cos(2\tau_c)\sin(\frac{\pi/2-2\theta_0}{2^{k_\theta}-1}) = \sin(\frac{\tau_c}{2^{k_\tau}-1})$, *and* $p_0 = \frac{3}{\Omega_4}$ *with*

$$\Omega_4 \triangleq 3 + 6(2^{k_p} - 1)\sin(\frac{\Delta\tau}{2}) + 2(2^{k_p} - 1)(2^{k_p+1} - 1)\sin^2(\frac{\Delta\tau}{2}),$$

and $\Delta p = 2\sqrt{p_0}\sin(\frac{\Delta\tau}{2})$. *In such a case,* $d_{R_1}(k_p, k_\tau, k_\theta, k_\phi) = \Delta p$.

9. *when* $k_\tau \neq 0$, $k_p = 0$, $k_\theta \neq 0$, *and* $k_\phi \neq 0$: $p_0 = 1$; θ_0 *is the solution to the equation* $\sin(2\theta_0)\sin(\frac{\pi}{2^{k_\phi}}) = \sin(\frac{\pi/2-2\theta_0}{2^{k_\theta}-1})$; $\tau_c \in [0, \frac{\pi}{4})$ *is the solution to the equation* $\cos(2\tau_c)\sin(\frac{\pi/2-2\theta_0}{2^{k_\theta}-1}) = \sin(\frac{\tau_c}{2^{k_\tau}-1})$. *In such a case,* $d_{R_1}(k_p, k_\tau, k_\theta, k_\phi) = 2\sin(\frac{\Delta\tau}{2})$.
10. *when* $k_\tau \neq 0$, $k_p \neq 0$, $k_\theta = 0$, *and* $k_\phi \neq 0$: $\theta_0 = \frac{\pi}{4}$; $\tau_c \in [0, \frac{\pi}{4})$ *is the solution to the equation* $\cos(2\tau_c)\sin(\frac{\pi}{2^{k_\phi}}) = \sin\frac{\tau_c}{2^{k_\tau}-1}$. $p_0 = \frac{3}{\Omega_4}$ *and* $\Delta p = 2\sqrt{p_0}\sin(\frac{\Delta\tau}{2})$. *In such a case,* $d_{R_1}(k_p, k_\tau, k_\theta, k_\phi) = \Delta p$.

11. *when* $k_\tau \neq 0$, $k_p \neq 0$, $k_\theta \neq 0$, *and* $k_\phi = 0$*:* $\theta_0 = 0$*;* $\tau_c \in [0, \frac{\pi}{4})$ *is the solution to the equation* $\cos(2\tau_c)\sin(\frac{\pi/2-2\theta_0}{2^{k_\theta}-1}) = \sin(\frac{\tau_c}{2^{k_\tau}-1})$*.* $p_0 = \frac{3}{\Omega_4}$ *and* $\Delta p = 2\sqrt{p_0}\sin(\frac{\Delta\tau}{2})$*. In such a case,* $d_{R_1}(k_p, k_\tau, k_\theta, k_\phi) = 2\sqrt{p_0}\sin(\frac{\Delta\tau}{2})$*.*
12. *when* $k_\tau \neq 0$, $k_p \neq 0$, $k_\theta = 0$, *and* $k_\phi = 0$*:* $\tau_c = \frac{\pi}{4}$*;* $p_0 = \frac{3}{\Omega_4}$ *and* $\Delta p = 2\sqrt{p_0}\sin(\frac{\Delta\tau}{2})$*. In such a case,* $d_{R_1}(k_p, k_\tau, k_\theta, k_\phi) = 2\sqrt{p_0}\sin(\frac{\Delta\tau}{2})$*.*
13. *when* $k_\tau \neq 0$, $k_p = 0$, $k_\theta \neq 0$, *and* $k_\phi = 0$*:* $p_0 = 1$ *and* $\Delta p = 0$*;* $\theta_0 = 0$*;* $\tau_c \in [0, \frac{\pi}{4})$ *is the solution to the equation* $\cos(2\tau_c)\sin(\frac{\pi/2-2\theta_0}{2^{k_\theta}-1}) = \sin(\frac{\tau_c}{2^{k_\tau}-1})$*. In such a case,* $d_{R_1}(k_p, k_\tau, k_\theta, k_\phi) = 2\sin(\frac{\Delta\tau}{2})$*.*
14. *when* $k_\tau \neq 0$, $k_p = 0$, $k_\theta = 0$, *and* $k_\phi \neq 0$*:* $p_0 = 1$ *and* $\Delta p = 0$*;* $\theta_c = \frac{\pi}{4}$*;* $\tau_c \in [0, \frac{\pi}{4})$ *is the solution to the equation* $\cos(2\tau_c)\sin(\frac{\pi}{2^{k_\phi}}) = \sin\frac{\tau_c}{2^{k_\tau}-1}$*. In such a case,* $d_{R_1}(k_p, k_\tau, k_\theta, k_\phi) = 2\sin(\frac{\Delta\tau}{2})$*.*
15. *when* $k_\tau \neq 0$, $k_p = 0$, $k_\theta = 0$, *and* $k_\phi = 0$*:* $p_0 = 1$ *and* $\Delta p = 0$*;* $\theta_0 = \frac{\pi}{4}$*;* $\tau_c = \frac{\pi}{4}$*. In such a case,* $d_{R_1}(k_p, k_\tau, k_\theta, k_\phi) = 2\sin(\frac{\Delta\tau}{2})$*.*

The proof of Proposition 2 is provided in Appendix B.

3.3. Optimization of Cardinality for Each Sub-constellation

After that, the optimal constellation size can be further attained by

$$\begin{aligned} \{\hat{k}_p, \hat{k}_\tau, \hat{k}_\theta, \hat{k}_\phi\} = \arg \max_{k_p, k_\tau, k_\theta, k_\phi} & \, d_{R_1}(k_p, k_\tau, k_\theta, k_\phi) \\ s.t. \; & k_p + k_\tau + k_\theta + k_\phi = 2L. \\ & k_p \in \mathbb{Z}_0^+, k_\tau \in \mathbb{Z}_0^+, k_\theta \in \mathbb{Z}_0^+, k_\phi \in \mathbb{Z}_0^+. \end{aligned} \tag{17}$$

where $\mathbb{Z}_0^+$ denotes the set for non-negative integers. L is the data transmission rate per channel use, i.e. $L = \frac{\log_2 |\mathcal{S}|}{2}$. An exhaustive search scheme can efficiently solve this optimization problem. In Table 1, we provide the optimal cardinality of each sub-constellation and corresponding constellation parameters for our proposed coding scheme $\mathcal{S}$. From Table 1, we can observe that the regular structure of our proposed constellation enables the transmitter and the receiver to generate a complete constellation of various sizes by just using 10 parameters, i.e., $k_p, k_\tau, k_\theta, k_\phi$ and $\{p_0, \Delta p, \tau_c, \Delta\tau, \theta_0, \Delta\theta\}$, which is a practical merit for the proposed code.

In Figure 1, we compare the achieved RD of our proposed scheme with the MUFC scheme under the same data transmission rate. From Figure 1, it shows that our proposed scheme has a larger RD than the MUFC coding scheme in [14] when the cardinality of $\mathcal{S}$ is larger than 16.

Table 1: Optimum modulation orders and key parameters for sub-constellations

L	Optimum $(k_p, k_\tau, k_\theta, k_\phi)$	Key Parameters in optimal $\mathcal{P}, \mathcal{T}, \Theta, \Phi$	$d_{R_1}(k_p, k_\tau, k_\theta, k_\phi)$
0.5	$(0,0,0,1)$	$p_0 = 1, \Delta p = 0; \tau_c = 0, \Delta\tau = 0; \theta_0 = \frac{\pi}{4}, \Delta\theta = 0; \Phi =$BPSK.	1.4142
1	$(0,0,0,2)$	$p_0 = 1, \Delta p = 0; \tau_c = 0, \Delta\tau = 0; \theta_0 = \frac{\pi}{4}, \Delta\theta = 0; \Phi =$ 4PSK.	0.7654
1.5	$(0,0,1,2)$	$p_0 = 1, \Delta p = 0; \tau_c = 0, \Delta\tau = 0; \theta_0 = 0.4777, \Delta\theta = 0.6154;\ \Phi =$ 4PSK.	0.6058
2	$(1,0,1,2)$	$p_0 = 0.5589, \Delta p = 0.4529; \tau_c = 0, \Delta\tau = 0; \theta_0 = 0.4777, \Delta\theta = 0.6154;\ \Phi =$ 4PSK.	0.4529
2.5	$(1,1,1,2)$	$p_0 = 0.6728, \Delta p = 0.3318;\ \tau_c = 0.4073, \Delta\tau = 0.4073;\ \theta_0 = 0.4777, \Delta\theta = 0.6154;\ \Phi =$ 4PSK.	0.3318
3	$(1,1,1,3)$	$p_0 = 0.7446, \Delta p = 0.2576; \tau_c = 0.2996, \Delta\tau = 0.2996;\ \theta_0 = 0.6027, \Delta\theta = 0.3655;\ \Phi =$ 8PSK.	0.2576
3.5	$(1,1,2,3)$	$p_0 = 0.7902, \Delta p = 0.2110; \tau_c = 0.2380, \Delta\tau = 0.2380;\ \theta_0 = 0.3828, \Delta\theta = 0.2684;\ \Phi =$ 8PSK.	0.2110
4	$(2,1,2,3)$	$p_0 = 0.5237, \Delta p = 0.1343;\ \tau_c = 0.1718, \Delta\tau = 0.2380;\ \theta_0 = 0.3828, \Delta\theta = 0.2684;\ \Phi =$ 8PSK.	0.1718
4.5	$(2,1,2,4)$	$p_0 = 0.6342, \Delta p = 0.1288; \tau_c = 0.1619, \Delta\tau = 0.1619;\ \theta_0 = 0.5291, \Delta\theta = 0.1709;\ \Phi =$ 16PSK.	0.1288
5	$(2,2,2,4)$	$p_0 = 0.6999, \Delta p = 0.1044; \tau_c = 0.3745, \Delta\tau = 0.1248;\ \theta_0 = 0.5291, \Delta\theta = 0.1709;\ \Phi =$ 16PSK.	0.1044

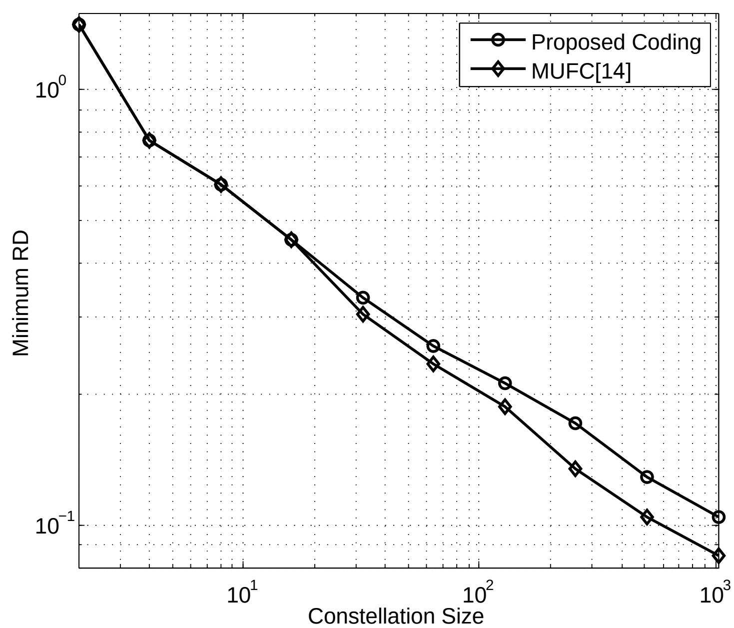

Figure 1: The achieved minimum RD distance compared with [14].

4. Low Complexity RD-based Receiver

The proposed RD-based receiver in (6) needs to calculate the objective function value 4^L times to determine the final result. However, there exists a low-complexity algorithm.

Let us denote $\mathbf{\Psi} = \frac{\tilde{\mathbf{Y}}^H \tilde{\mathbf{Y}}}{M} - \frac{\text{tr}\{\mathbf{\Sigma}^{-1}\}}{M}\sigma_n^2 \mathbf{I}_2 = \begin{pmatrix} \psi_{11} & \psi_{12} \\ \psi_{12}^* & \psi_{22} \end{pmatrix}$, $\mathbf{\Psi}^H = \mathbf{\Psi}$. Then the RD-based Receiver can be built as

$$\begin{aligned}\hat{\mathbf{S}} &= \arg\min_{\mathbf{S}\in\mathcal{S}} \mathrm{tr}\{\boldsymbol{\Psi}\} + \mathrm{tr}\{\mathbf{S}^H\mathbf{S}\} - 2\mathrm{tr}\{(\boldsymbol{\Psi}\mathbf{S}^H\mathbf{S})^{\frac{1}{2}}\} \\ &= \arg\min_{\mathbf{S}\in\mathcal{S}} \mathrm{tr}\{\mathbf{S}^H\mathbf{S}\} - 2\sqrt{\mathrm{tr}\{\boldsymbol{\Psi}\mathbf{S}^H\mathbf{S}\} + 2(\det(\boldsymbol{\Psi}\mathbf{S}^H\mathbf{S}))^{\frac{1}{2}}}, \end{aligned} \tag{18}$$

where

$$\boldsymbol{\Psi}\mathbf{S}^H\mathbf{S} = \begin{pmatrix} \psi_{11} & \psi_{12} \\ \psi_{12}^* & \psi_{22} \end{pmatrix} \begin{pmatrix} a^2\cos^2\theta + b^2\sin^2\theta & (a^2-b^2)e^{j\phi}\sin\theta\cos\theta \\ (a^2-b^2)e^{-j\phi}\sin\theta\cos\theta & a^2\sin^2\theta + b^2\cos^2\theta \end{pmatrix}. \tag{19}$$

Then,

$$\mathrm{tr}\{\boldsymbol{\Psi}\mathbf{S}^H\mathbf{S}\} = \frac{p}{2}(\psi_{11}+\psi_{22}) + p\cos(2\tau)\Big[\frac{\psi_{11}-\psi_{22}}{2}\cos(2\theta) + \Re\{\psi_{12}e^{-j\phi}\}\sin(2\theta)\Big], \tag{20}$$

$$\det\{\boldsymbol{\Psi}\mathbf{S}^H\mathbf{S}\} = p\cos^2(\tau)\sin^2(\tau)(\psi_{11}\psi_{22} - |\psi_{12}|^2). \tag{21}$$

Finally, we have

$$\begin{aligned}\{\hat{p},\hat{\tau},\hat{\theta},\hat{\phi}\} &\overset{(a)}{=} \arg\min_{\sqrt{p}\in\mathcal{P},\tau\in\mathcal{T},\theta\in\Theta,e^{j\phi}\in\Phi} p - 2\sqrt{p}\Big(\frac{1}{2}(\psi_{11}+\psi_{22}) \\ &\quad + \cos(2\tau)\Big[\frac{\psi_{11}-\psi_{22}}{2}\cos(2\theta) + \Re\{\psi_{12}e^{-j\phi}\}\sin(2\theta)\Big] \\ &\quad + \sin(2\tau)\sqrt{\psi_{11}\psi_{22}-|\psi_{12}|^2}\Big)^{\frac{1}{2}} \\ &\overset{(b)}{=} \arg\min_{\sqrt{p}\in\mathcal{P},\tau\in\mathcal{T},\theta\in\Theta,e^{j\phi}\in\Phi} p - 2\sqrt{p}\Big(\frac{1}{2}(\psi_{11}+\psi_{22}) \\ &\quad + \cos(2\tau)\sqrt{(\frac{\psi_{11}-\psi_{22}}{2})^2 + \Re^2\{\psi_{12}e^{-j\phi}\}}\sin(2\theta+\eta) \\ &\quad + \sin(2\tau)\sqrt{\psi_{11}\psi_{22}-|\psi_{12}|^2}\Big)^{\frac{1}{2}} \\ &\overset{(c)}{=} \arg\min_{\sqrt{p}\in\mathcal{P},\tau\in\mathcal{T},\theta\in\Theta,e^{j\phi}\in\Phi} p - 2\sqrt{p}\Big(\frac{1}{2}(\psi_{11}+\psi_{22}) + \sqrt{t_1^2+t_2^2}\cos(2\tau-\xi)\Big)^{\frac{1}{2}}, \end{aligned} \tag{22}$$

where $\tan\eta = \frac{\psi_{11}-\psi_{22}}{2\Re\{\psi_{12}e^{-j\hat{\phi}}\}}$, $t_1 = \frac{\psi_{11}-\psi_{22}}{2}\cos(2\hat{\theta}) + \Re\{\psi_{12}e^{-j\hat{\phi}}\}\sin(2\hat{\theta})$ and $t_2 = \sqrt{\psi_{11}\psi_{22} - |\psi_{12}|^2}$, $\tan\xi = \frac{t_2}{t_1}$.

We can estimate ϕ with $\hat{\phi} = \arg\max_{e^{j\phi}\in\Phi} \Re\{\psi_{12}e^{-j\phi}\}$ from the equality (a); From the equality (b), we can estimate θ with

$$\hat{\theta} = \arg\min_{\theta\in\Theta} \left|\theta - (\frac{\pi}{4} - \frac{1}{2}\arctan\frac{\psi_{11}-\psi_{22}}{2\Re\{\psi_{12}e^{-j\hat{\phi}}\}})\right|. \tag{23}$$

From the equality (c), we can first estimate τ with

$$\hat{\tau} = \arg\min_{\tau\in\mathcal{T}} |\tau - \frac{1}{2}\xi|. \tag{24}$$

and then estimate p with

$$\hat{p} = \arg\min_{\sqrt{p}\in\mathcal{P}} \left|p - \left(\frac{1}{2}(\psi_{11}+\psi_{22}) \ + \sqrt{t_1^2+t_2^2}\cos(2\hat{\tau}-\xi)\right)^{\frac{1}{2}}\right|. \tag{25}$$

Based on the above discussion, we can summarize our proposed low-complexity RD-based receiver as Algorithm 1. With Algorithm 1, we can attain that the proposed algorithm only needs to calculate $2^{k_p}+2^{k_\tau}+2^{k_\theta}+2^{k_\phi}$ times, which is of lower complexity than the original receiver built in (6).

5. Simulation Results

We apply an exponential decaying correlation model [23] in our simulations. In detail, the (m,n)-th entry of the correlation matrix of $\mathbf{R}$ is generated by $[\mathbf{R}]_{m,n} = \gamma^{|m-n|}$, where $0 < \gamma < 1$. The SNR in all simulations is defined by SNR$\triangleq \frac{\mathbb{E}\{\mathrm{tr}\{\mathbf{S}^H\mathbf{S}\}\}}{2\sigma_0^2}$.

In this section, we conduct a series of computer simulations to verify the performance of our proposed scheme further. First, we study the proposed scheme's symbol error rate (SER) compared with the MUFC scheme proposed in [14] at $L = 2.5$bits per channel use in Figure 2. To make a fair comparison, we assume the MUFC uses the same RD detector (6) for decoding. From Figure 2, we can see that the proposed scheme is superior to the MUFC coding scheme when M is larger than 16 for both $\gamma = 0.1$ and $\gamma = 0.5$. Also, the performance gap enlarges when the SNR increases from 10dB to 20dB.

Algorithm 1 Proposed Low-complexity RD-based Detector

Input: $\mathbf{Y}$, $\mathbf{U}_R$, $\boldsymbol{\Sigma}$, $\hat{\mathcal{P}}$, $\hat{\mathcal{T}}$, $\hat{\Theta}$, and $\hat{\Phi}$.
Output: $\hat{\phi}$, $\hat{\theta}$, $\hat{\tau}$, and $\hat{p}$;

```
Calculate $\tilde{\mathbf{Y}} = \boldsymbol{\Sigma}^{-\frac{1}{2}}\mathbf{U}_R^H\mathbf{Y}$, $\boldsymbol{\Psi} = \frac{\tilde{\mathbf{Y}}^H\tilde{\mathbf{Y}}}{M} - \frac{\mathrm{tr}\{\boldsymbol{\Sigma}^{-1}\}}{M}\sigma_n^2\mathbf{I}_2 = [\psi_{11}, \psi_{12}; \psi_{21}, \psi_{22}]$.
if $k_\phi \neq 0$ then
    $\hat{\phi} = \arg\max_{e^{j\phi}\in\Phi} \Re\{\psi_{12}e^{-j\phi}\}$;
else
    $\hat{\phi} = 0$
end if
if $k_\theta \neq 0$ then
    $\hat{\theta} = \arg\min_{\theta\in\Theta} \left|\theta - \left(\frac{\pi}{4} - \frac{1}{2}\arctan\frac{\psi_{11}-\psi_{22}}{2\Re\{\psi_{12}e^{-j\hat{\phi}}\}}\right)\right|$.
else
    $\hat{\theta} = \frac{\pi}{4}$;
end if
Calculate $t_1 = \frac{\psi_{11}-\psi_{22}}{2}\cos(2\hat{\theta}) + \Re\{\psi_{12}e^{-j\hat{\phi}}\}\sin(2\hat{\theta})$ ,
$t_2 = \sqrt{\psi_{11}\psi_{22} - |\psi_{12}|^2}$, and $\xi = \arctan\frac{t_2}{t_1}$.
if $k_\tau \neq 0$ then
    $\hat{\tau} = \arg\min_{\tau\in\mathcal{T}} |\tau - \frac{1}{2}\xi|$.
else
    $\hat{\tau} = 0$;
end if
if $k_p \neq 0$ then
    $\hat{p} = \arg\min_{\sqrt{p}\in\mathcal{P}} \left|p - \left(\frac{1}{2}(\psi_{11} + \psi_{22}) + \sqrt{t_1^2 + t_2^2}\cos(2\hat{\tau} - \xi)\right)^{\frac{1}{2}}\right|$.
else
    $\hat{p} = 1$.
end if
return $\hat{\phi}, \hat{\theta}, \hat{\tau}$, and $\hat{p}$.
```

In Figure 3, we compare our proposed scheme with the scheme proposed in [12] with M increasing when $\gamma = 0.1$ and $\gamma = 0.5$, respectively. In [12], $\mathbf{S}$ is constructed by PSK constellation symbols. In detail, $\mathbf{S} = \frac{1}{\sqrt{2}} \begin{bmatrix} 1 & x^* \\ x & 1 \end{bmatrix}$, where x is randomly chosen from 4^L-PSK constellations. For the sake of fair comparison, we also assume the detector used at the BS for [12] is the RD detector proposed in (6). From Figure 3, we observe that our proposed scheme has a significant advantage over the scheme in [12], especially when the SNR is low.

In Figure 4, we study the SER performance of our proposed scheme when the correlation factor γ varies from $\gamma = 0.1$ to $\gamma = 0.5$. Also, we provide the performance of MUFC [14] and PSK scheme [12] for comparison. In this figure, M= 128, SNR=10dB, $L = 2.5$bits/channel use. Figure 4 shows that the SER of our proposed scheme degrades with γ increasing. This phenomenon indicates that to extend the work to the case with more than two transmitter antennas, one possible way is to use antenna selection based on the knowledge of the correlation coefficient. Also, we can observe that the SER of our proposed scheme is better than MUFC and PSK scheme. Also, we note the performance gap with the MUFC scheme decreases with γ increasing. Finally, in Figure 5, we investigate the SER performance of our proposed scheme with L varying when M= 128, SNR= $10dB$ and $\gamma = 0.3$. Since Table 1 shows when $L \leq 2$, the MUFC scheme is equivalent to our proposed scheme, we only provide the results when $L \geq 2.5$. From Figure 5, we can attain that our proposed scheme has a superior error performance to the PSK modulation scheme proposed in [12] and the MUFC scheme in [14].

In Figure 6, we investigate the diversity gain (the slope of SER curves) of our proposed scheme through the simulation results. We observe error floors for our proposed scheme in the high SNR scenario. With M increasing, the error floors tend to vanish. This phenomenon is mainly because our proposed scheme relies on the assumption of asymptotic orthogonality property in massive MIMO systems.

6. Conclusion

In this paper, we have investigated a massive MIMO uplink system in correlated Rayleigh fading channels, in which a transmitter with two antennas needs to upload data timely to a BS having a larger number of antennas. We have built a modified RD-based detector and a novel parametric space-time coding scheme for such a system. Analytical results are derived for optimal constellation structural and optimal modulation orders. The attained results show that by using more antennas, the RD can be increased by using more antennas compared with a single antenna. Also, we have proved that our proposed noncoherent constellation enables a fast decoding algorithm. Finally, various simulation results have shown that our proposed scheme performs superior to the MUFC and PSK modulation systems.

Acknowledgments

The work of S. Li was supported in part by the National Natural Science Foundation of China under Grant No. 61901416; in part by the China Postdoctoral Science Foundation under Grant No. 2021TQ0304. The work of X. Guo was supported in part by the National Natural Science Foundation of China under Grant No. 62101503; in part by the Henan Postdoctoral Research Grant (No. 1902012).

Appendix A. Proof of Proposition 1

Since

$$\mathbb{E}\Big\{\|\frac{\tilde{\mathbf{Y}}^H\tilde{\mathbf{Y}}}{M}-\mathbf{A}\|_F^2\Big\} \quad =\mathbb{E}\Big\{\frac{1}{M^2}\,\mathrm{tr}\{(\tilde{\mathbf{Y}}^H\tilde{\mathbf{Y}})^2\}-\frac{2}{M}\,\mathrm{tr}\{\tilde{\mathbf{Y}}^H\tilde{\mathbf{Y}}\mathbf{A}\}+\mathrm{tr}\{\mathbf{A}^2\}\Big\}, \tag{A.1}$$

where $\tilde{\mathbf{Y}}^H\tilde{\mathbf{Y}}=\mathbf{S}^H\tilde{\mathbf{H}}^H\tilde{\mathbf{H}}\mathbf{S}+\mathbf{S}^H\tilde{\mathbf{H}}^H\tilde{\mathbf{N}}+\tilde{\mathbf{N}}^H\tilde{\mathbf{H}}\mathbf{S}+\tilde{\mathbf{N}}^H\tilde{\mathbf{N}}$.

Thus, we can attain

$$\mathbb{E}\Big\{\,\mathrm{tr}\{\tilde{\mathbf{Y}}^H\tilde{\mathbf{Y}}\mathbf{A}\}\Big\}=M\,\mathrm{tr}\,\Big\{(\mathbf{S}^H\mathbf{S}+\frac{\mathrm{tr}\{\mathbf{\Sigma}^{-1}\}}{M}\sigma_n^2\mathbf{I}_2)\mathbf{A}\Big\}, \tag{A.2}$$

$$\begin{aligned}\mathbb{E}\Big\{\,\mathrm{tr}\{(\tilde{\mathbf{Y}}^H\tilde{\mathbf{Y}})^2\}\Big\}&=\mathbb{E}\Big\{\,\mathrm{tr}\{\mathbf{S}^H\tilde{\mathbf{H}}^H\tilde{\mathbf{H}}\mathbf{S}\mathbf{S}^H\tilde{\mathbf{H}}^H\tilde{\mathbf{H}}\mathbf{S}\}\Big\}+2\mathbb{E}\Big\{\,\mathrm{tr}\{\mathbf{S}^H\tilde{\mathbf{H}}^H\tilde{\mathbf{H}}\mathbf{S}\tilde{\mathbf{N}}^H\tilde{\mathbf{N}}\}\Big\}\\&+2\mathbb{E}\Big\{\,\mathrm{tr}\{\tilde{\mathbf{N}}^H\tilde{\mathbf{H}}\mathbf{S}\mathbf{S}^H\tilde{\mathbf{H}}^H\tilde{\mathbf{N}}\}\Big\}+\mathbb{E}\Big\{\,\mathrm{tr}\{\tilde{\mathbf{N}}^H\tilde{\mathbf{N}}\tilde{\mathbf{N}}^H\tilde{\mathbf{N}}\}\Big\}\\&=M^2\mathrm{tr}\{(\mathbf{S}^H\mathbf{S}+\frac{\mathrm{tr}\{\mathbf{\Sigma}^{-1}\}}{M}\sigma_n^2\mathbf{I}_2)^2\}+M\mathrm{tr}^2\{\mathbf{S}^H\mathbf{S}\}+\mathrm{tr}\{\mathbf{\Sigma}^{-2}\}\mathrm{tr}^2(\sigma_n^2\mathbf{I}_2)\\&+2M\mathrm{tr}\{\mathbf{S}^H\mathbf{S}\}\mathrm{tr}\{\frac{\mathrm{tr}\{\mathbf{\Sigma}^{-1}\}}{M}\sigma_n^2\mathbf{I}_2\}.\end{aligned} \tag{A.3}$$

Finally, we arrive at

$$\begin{aligned}&\mathbb{E}\{\|\frac{\tilde{\mathbf{Y}}^H\tilde{\mathbf{Y}}}{M}-\mathbf{A}\|_F^2\}\\&=\mathrm{tr}\left\{(\mathbf{S}^H\mathbf{S}+\frac{\mathrm{tr}\{\mathbf{\Sigma}^{-1}\}}{M}\sigma_n^2\mathbf{I}_2-\mathbf{A})^2\right\}+\mathbf{\Delta},\end{aligned} \tag{A.4}$$

where $\mathbf{\Delta}=\frac{1}{M}\mathrm{tr}^2\{\mathbf{S}^H\mathbf{S}\}+\frac{1}{M^2}\mathrm{tr}\{\mathbf{\Sigma}^{-2}\}\mathrm{tr}^2(\sigma_n^2\mathbf{I}_2)+\frac{2}{M}\mathrm{tr}\{\mathbf{S}^H\mathbf{S}\}\mathrm{tr}\{\frac{\mathrm{tr}\{\mathbf{\Sigma}^{-1}\}}{M}\sigma_n^2\mathbf{I}_2\}$. When $M\to\infty$, we can conclude

$$\arg\min_{\mathbf{A}}\lim_{M\to\infty}\mathbb{E}\{\|\frac{\tilde{\mathbf{Y}}^H\tilde{\mathbf{Y}}}{M}-\mathbf{A}\|_F^2\}=\mathbf{S}^H\mathbf{S}+\frac{\mathrm{tr}\{\mathbf{\Sigma}^{-1}\}}{M}\sigma_n^2\mathbf{I}_2. \tag{A.5}$$

This completes the proof of Proposition 1.

Appendix B. Proof of Proposition 2

Let $J(k_p,k_\tau,k_\theta,k_\phi)\triangleq\min_{(p_i,\tau_i,\theta_i,\phi_i)\neq(p_j,\tau_j,\theta_j,\phi_j)}\mathrm{tr}\{\mathbf{S}_i^H\mathbf{S}_i\}+\mathrm{tr}\{\mathbf{S}_j^H\mathbf{S}_j\}-2\mathrm{tr}\{(\mathbf{S}_i^H\mathbf{S}_i\mathbf{S}_j^H\mathbf{S}_j)^{\frac{1}{2}}\}$, then, we have $d_{R_1}(k_p,k_\tau,k_\theta,k_\phi)=\max\sqrt{J(k_p,k_\tau,k_\theta,k_\phi)}$. For $k_\tau=0$, if $\tau_i=\tau_j=\tau_c$ (τ_c is a variable within $[0,\frac{\pi}{4})$), we attain

$$\begin{aligned}J(k_p,k_\tau,&k_\theta,k_\phi)=\min_{(p_i,\theta_i,\phi_i)\neq(p_j,\theta_j,\phi_j)}\\&p_i+p_j-2\sqrt{p_ip_j}\times\sqrt{1+\cos^2(2\tau_c)(\Xi(\theta_i,\theta_j,\phi_i,\phi_j)-1)},\end{aligned} \tag{B.1}$$

where

$$\begin{aligned}&\Xi(\theta_i,\theta_j,\phi_i,\phi_j)\\&=\cos^2\theta_i\cos^2\theta_j+\sin^2\theta_i\sin^2\theta_j+2\sin\theta_i\cos\theta_i\sin\theta_j\cos\theta_j\cos(\phi_i-\phi_j)\\&\overset{(a)}{\leq}\cos^2\theta_i\cos^2\theta_j+\sin^2\theta_i\sin^2\theta_j+2\sin\theta_i\cos\theta_i\sin\theta_j\cos\theta_j\\&\overset{(b)}{\leq}1,\end{aligned} \tag{B.2}$$

where the equality in (a) holds when $\phi_i=\phi_j$, the equality in (b) holds when $\theta_i=\theta_j$. Therefore, we conclude that when $\tau_c=0$, (B.1) can be maximized. This indicates that using a single antenna is better than using two antennas when $k_\tau=0$. In such a case, the coding scheme degrades to the MUFC scheme proposed in [14], where

$$J(k_p, k_\tau, k_\theta, k_\phi) = \min_{(p_i,\theta_i,\phi_i)\neq(p_j,\theta_j,\phi_j)} p_i + p_j \\ - \sqrt{2p_ip_j}\sqrt{1+\cos(2\theta_i)\cos(2\theta_j)+\sin(2\theta_i)\sin(2\theta_j)\cos(\phi_i-\phi_j)}. \quad \text{(B.3)}$$

Based on [14], we can attain the results for 1-7 cases in Proposition 2.

For the rest cases, we only need to consider the cases when $k_\tau \neq 0$. To determine the optimal $\mathcal{S}$, we first determine the closed-form of $J(k_p, k_\tau, k_\theta, k_\phi)$ when $k_\tau \neq 0$, then use the max-min rule to determine the optimal structure of $\mathcal{S}$.

In line with this, we first consider the case when k_ϕ, k_θ, and k_p are positive integers. In such a case, the global minimum value of $J(k_p, k_\tau, k_\theta, k_\phi)$ can be attained by comparing the following five items:

$$\begin{cases} J(p_i \neq p_j, (\tau_i,\theta_i,\phi_i) = (\tau_j,\theta_j,\phi_j)), \\ J(p_i \neq p_j, (\tau_i,\theta_i,\phi_i) \neq (\tau_j,\theta_j,\phi_j)), \\ J(p_i = p_j, \tau_i \neq \tau_j, (\theta_i,\phi_i) = (\theta_j,\phi_j)), \\ J(p_i = p_j, \tau_i \neq \tau_j, (\theta_i,\phi_i) \neq (\theta_j,\phi_j)), \\ J(p_i = p_j, \tau_i = \tau_j, (\theta_i,\phi_i) \neq (\theta_j,\phi_j)). \end{cases}$$

Since

$$J(p_i \neq p_j, (\tau_i,\theta_i,\phi_i) = (\tau_j,\theta_j,\phi_j)) < J(p_i \neq p_j, (\tau_i,\theta_i,\phi_i) \neq (\tau_j,\theta_j,\phi_j)), \\ J(p_i = p_j, \tau_i \neq \tau_j, (\theta_i,\phi_i) = (\theta_j,\phi_j)) < J(p_i = p_j, \tau_i \neq \tau_j, (\theta_i,\phi_i) \neq (\theta_j,\phi_j)),$$

$J(k_p, k_\tau, k_\theta, k_\phi)$ can be further constrained in the following three items:

$$J(p_i \neq p_j, (\tau_i,\theta_i,\phi_i) = (\tau_j,\theta_j,\phi_j)), \quad \text{(B.4a)}$$

$$J(p_i = p_j, \tau_i \neq \tau_j, (\theta_i,\phi_i) = (\theta_j,\phi_j)), \quad \text{(B.4b)}$$

$$J((p_i,\tau_i) = (p_j,\tau_j), (\theta_i,\phi_i) \neq (\theta_j,\phi_j)). \quad \text{(B.4c)}$$

We observe that the structure of Θ and Φ only affect (B.5) with

$$J((p_i,\tau_i) = (p_j,\tau_j) = (p_t,\tau_c), (\theta_i,\phi_i) \neq (\theta_j,\phi_j)) \\ = \min_{p_t,\tau_c,(\theta_i,\phi_i)\neq(\theta_j,\phi_j)} 2p_t - 2p_t \times \sqrt{1+\cos^2(2\tau_c)(\Xi(\theta_i,\theta_j,\phi_i,\phi_j)-1)}, \quad \text{(B.5)}$$

where p_t and τ_c are variables to be optimized. With the max-min rule, we can attain that the optimal Θ and Φ should ensure $\max_{(\theta_i,\phi_i)\neq(\theta_j,\phi_i)} \Xi(\theta_i,\theta_j,\phi_i,\phi_j)$

is minimal. Similar to the method in [14], we can attain $\hat{\Phi} = 2^{k_\phi}$-PSK, $\hat{\Theta} = \{\theta_0 + i\Delta\theta\}_{i=0}^{2^{k_\theta}-1}$ with θ_0 $(0 < \theta_0 < \frac{\pi}{4})$ being the solution to $\sin(2\theta_0)\sin(\frac{\pi}{2^{k_\phi}}) = \sin(\frac{\pi/2-2\theta_0}{2^{k_\theta}-1})$ and $\Delta\theta = \frac{\pi/2-2\theta_0}{2^{k_\theta}-1}$. With the optimal θ_0, we attain

$$\max_{(\theta_i,\phi_i)\neq(\theta_j,\phi_j)} \Xi(\theta_i,\theta_j,\phi_i,\phi_j) = \cos^2(\frac{\pi/2-2\theta_0}{2^{k_\theta}-1}). \tag{B.6}$$

Since the structure of $\mathcal{T}$ only affects (B.7) with

$$J(p_i = p_j = p_t, \tau_i \neq \tau_j, (\theta_i,\phi_i) = (\theta_j,\phi_j)) = \min_{p_t,\tau_i\neq\tau_j} 2p_t - 2p_t\cos(\tau_i - \tau_j), \tag{B.7}$$

we can conclude that the optimal $\mathcal{T}$ is an arithmetic sequence. i.e., $\mathcal{T} = \{0, \Delta\tau, \cdots, \tau_c\}$ with $\Delta\tau = \frac{\tau_c}{2^{k_\tau}-1}$. Then, we can simplify (B.7) as

$$J(p_i = p_j, \tau_i \neq \tau_j, (\theta_i,\phi_i) = (\theta_j,\phi_j)) = \min_{p_t} 2p_t - 2p_t\cos(\frac{\tau_c}{2^{k_\tau}-1}), \tag{B.8}$$

Also, since $\tau_c \in [0, \frac{\pi}{4})$, we can simplify (B.5)

$$\begin{aligned} &J((p_i,\tau_i) = (p_j,\tau_j), (\theta_i,\phi_i) \neq (\theta_j,\phi_j)) \\ &= \min_{p_t} 2p_t - 2p_t \times \sqrt{1 - \cos^2(2\tau_c)\sin^2(\frac{\pi/2-2\theta_0}{2^{k_\theta}-1})}, \end{aligned} \tag{B.9}$$

By jointly maximizing (B.8) and (B.9) concerning τ_c, we can attain the optimal τ_c by solving (B.10),

$$\begin{aligned} &J(p_i = p_j = p_t, \tau_i \neq \tau_j, (\theta_i,\phi_i) = (\theta_j,\phi_j)) \\ &= J(p_i = p_j = p_t, \tau_i = \tau_j = \tau_c, (\theta_i,\phi_i) \neq (\theta_j,\phi_j)), \end{aligned} \tag{B.10}$$

which is equivalent to

$$\cos(2\tau_c)\sin(\frac{\pi/2-2\theta_0}{2^{k_\theta}-1}) = \sin(\frac{\tau_c}{2^{k_\tau}-1}), 0 \leq \tau_c < \frac{\pi}{4}. \tag{B.11}$$

With the optimal Θ, Φ, and $\mathcal{T}$, the minimum value between (B.4b) and (B.4c) can be maximized and equals to

$$\min_{p_t} 4p_t\sin^2(\frac{\Delta\tau}{2}). \tag{B.12}$$

Further, we find that the structure of $\mathcal{P}$ only affect $J(p_i \neq p_j, (\tau_i, \theta_i, \phi_i) = (\tau_j, \theta_j, \phi_j))$ with

$$J(p_i \neq p_j, (\tau_i, \theta_i, \phi_i) = (\tau_j, \theta_j, \phi_j)) = \min_{p_i \neq p_j} (\sqrt{p_i} - \sqrt{p_j})^2. \tag{B.13}$$

Using the max-min rule, we can conclude that the optimal $\mathcal{P}$ is also an arithmetic sequence $\mathcal{P} = \{\sqrt{p_0}, \sqrt{p_0} + \Delta p, \cdots, \sqrt{p_0} + (2^{k_p} - 1)\Delta p\}$. Then, by jointly maximizing (B.12) and (B.13), the optimal p_0 and Δp should satisfy

$$4p_0 \sin^2(\frac{\Delta\tau}{2}) = (\Delta p)^2. \tag{B.14}$$

Besides, considering the average power constraint for $\mathcal{P}$,

$$\sum_{i=0}^{2^{k_p}-1} [\sqrt{p_0} + i\Delta p]^2 = 2^{k_p}, \tag{B.15}$$

we can attain the optimal $p_0 = \frac{3}{\Omega_4}$ with

$$\Omega_4 \triangleq 3 + 6(2^{k_p} - 1)\sin(\frac{\Delta\tau}{2}) + 2(2^{k_p} - 1)(2^{k_p+1} - 1)\sin^2(\frac{\Delta\tau}{2}),$$

and $\Delta p = 2\sqrt{p_0}\sin(\frac{\Delta\tau}{2})$. Finally, with the optimal $\mathcal{P}$, $\mathcal{T}$, Θ, and Φ, we can attain $d_{R_1}(k_p, k_\tau, k_\theta, k_\phi) = 2\sqrt{p_0}\sin(\frac{\Delta\tau}{2})$. This completes the proof of case 8.

By referring to the proof process of case 8, we can derive the following conclusions for 9-15:

1. When one of k_p, k_θ, and k_ϕ is equal to zero, there exist three scenarios:
   (a) $k_p = 0$, $k_\theta \neq 0$, and $k_\phi \neq 0$: In this case, $J(k_p, k_\tau, k_\theta, k_\phi)$ is the minimum value between
   $$\begin{cases} J(p_i = p_j, \tau_i \neq \tau_j, (\theta_i, \phi_i) = (\theta_j, \phi_j)), \\ J((p_i, \tau_i) = (p_j, \tau_j), (\theta_i, \phi_i) \neq (\theta_j, \phi_j)). \end{cases}$$
   By jointly considering (B.5) and (B.7), we have the optimal $\mathcal{P} = \{1\}$, $\hat{\Phi} = 2^{k_\phi}$-PSK, and $\Theta = \{\theta_0 + i\Delta\theta\}_{i=0}^{2^{k_\theta}-1}$, with θ_0 $(0 < \theta_0 < \frac{\pi}{4})$ being the solution to $\sin(2\theta_0)\sin(\frac{\pi}{2^{k_\phi}}) = \sin(\frac{\pi/2 - 2\theta_0}{2^{k_\theta} - 1})$ and $\Delta\theta = \frac{\pi/2 - 2\theta_0}{2^{k_\theta} - 1}$. The optimal τ_c satisfies that (B.11). In such a case, we have $d_{R_1}(k_p, k_\tau, k_\theta, k_\phi) = 2\sin(\frac{\Delta\tau}{2})$. This completes the proof of case 9.

(b) $k_\theta = 0$, $k_p \neq 0$, and $k_\phi \neq 0$: In this case, $J(k_p, k_\tau, k_\theta, k_\phi)$ is the minimum value among $\begin{cases} J(p_i \neq p_j, (\tau_i, \theta_i, \phi_i) = (\tau_j, \theta_j, \phi_j)), \\ J(p_i = p_j, \tau_i \neq \tau_j, (\theta_i, \phi_i) = (\theta_j, \phi_j)), \\ J((p_i, \tau_i, \theta_i) = (p_j, \tau_j, \theta_j), \phi_i \neq \phi_j). \end{cases}$
By max-min rule, we attain the optimal $\Theta = \{\frac{\pi}{4}\}$, $\hat{\Phi} = 2^{k_\phi}$-PSK. $\mathcal{T} = \{0, \Delta\tau, \cdots, \tau_c\}$, where $\Delta\tau = \frac{\tau_c}{2^{k_\tau}-1}$. Specially, τ_c satisfies

$$\cos(2\tau_c)\sin(\frac{\Delta\phi}{2}) = \sin\frac{\tau_c}{2^{k_\tau}-1}. \tag{B.16}$$

The optimal $\mathcal{P} = \{\sqrt{p_0}, \sqrt{p_0}+\Delta p, \cdots, \sqrt{p_0}+(2^{k_p}-1)\Delta p\}$ with p_0 and Δp satisfying (B.14) and (B.15). Thus, we have $p_0 = \frac{3}{\Omega_4}$ and $\Delta p = 2\sqrt{p_0}\sin(\frac{\Delta\tau}{2})$. In such a case, we have $d_{R_1}(k_p, k_\tau, k_\theta, k_\phi) = 2\sqrt{p_0}\sin(\frac{\Delta\tau}{2})$. This completes the proof of case 10.

(c) $k_\phi = 0$, $k_p \neq 0$, and $k_\theta \neq 0$: In this case, $J(k_p, k_\tau, k_\theta, k_\phi)$ is the minimum value among
$\begin{cases} J(p_i \neq p_j, (\tau_i, \theta_i, \phi_i) = (\tau_j, \theta_j, \phi_j)), \\ J(p_i = p_j, \tau_i \neq \tau_j, (\theta_i, \phi_i) = (\theta_j, \phi_j)), \\ J((p_i, \tau_i, \phi_i) = (p_j, \tau_j, \phi_j), \theta_i \neq \theta_j), \end{cases}$
By max-min rule, we have the optimal $\Phi = \{1\}$, $\Theta = \{\theta_0 + i\Delta\theta\}_{i=0}^{2^{k_\theta}-1}$, where $\theta_0 = 0$ and $\Delta\theta = \frac{\pi/2}{2^{k_\theta}-1}$; The optimal $\mathcal{T} = \{0, \Delta\tau, \cdots, \tau_c\}$, where $\Delta\tau = \frac{\tau_c}{2^{k_\tau}-1}$. The optimal τ_c satisfies that

$$\cos(2\tau_c)\sin(\Delta\theta) = \sin\frac{\tau_c}{2^{k_\tau}-1}. \tag{B.17}$$

$\mathcal{P} = \{\sqrt{p_0}, \sqrt{p_0}+\Delta p, \cdots, \sqrt{p}_0+(2^{k_p}-1)\Delta p\}$, where p_0 and Δp satisfy $\sum_{i=0}^{2^{k_p}-1}[\sqrt{p_0}+i\Delta p]^2 = 2^{k_p}$ and $4p_0\sin^2(\frac{\Delta\tau}{2}) = (\Delta p)^2$. Thus, we have $p_0 = \frac{3}{\Omega_4}$ and $\Delta p = 2\sqrt{p_0}\sin(\frac{\Delta\tau}{2})$. In such a case, we have $d_{R_1}(k_p, k_\tau, k_\theta, k_\phi) = 2\sqrt{p_0}\sin(\frac{\Delta\tau}{2})$. This completes the proof of case 11.

2. When two of k_p, k_θ, and k_ϕ are equal to zeros, there exist three scenarios

(a) $k_p \neq 0$, $k_\theta = 0$, and $k_\phi = 0$: In this case, $J(k_p, k_\tau, k_\theta, k_\phi)$ is the minimum value between $\begin{cases} J(p_i \neq p_j, (\tau_i, \theta_i, \phi_i) = (\tau_j, \theta_j, \phi_j)), \\ J(p_i = p_j, \tau_i \neq \tau_j, (\theta_i, \phi_i) = (\theta_j, \phi_j)), \end{cases}$
By the max-min rule, the optimal $\Theta = \{\frac{\pi}{4}\}$, $\Phi = \{1\}$. The optimal $\mathcal{T} = \{0, \Delta\tau, \cdots, \frac{\pi}{4}\}$ with $\Delta\tau = \frac{\pi}{4(2^{k_\tau}-1)}$. The optimal $\mathcal{P} =$

$\{\sqrt{p_0}, \sqrt{p_0}+\Delta p, \cdots, \sqrt{p_{2^{k_p}-1}}\}$ under average power constraint $\sum_{i=0}^{2^{k_p}-1}(\sqrt{p_0}+i\Delta p)^2 = 2^{k_p}$ and $4p_0\sin^2(\frac{\Delta\tau}{2}) = (\Delta p)^2$. Thus, we have $p_0 = \frac{3}{\Omega_4}$ and $\Delta p = 2\sqrt{p_0}\sin(\frac{\Delta\tau}{2})$. In such a case, we have $d_{R_1}(k_p,k_\tau,k_\theta,k_\phi) = 2\sqrt{p_0}\sin(\frac{\Delta\tau}{2})$. This completes the case of 12.

(b) $k_\theta \neq 0$, $k_p = 0$, and $k_\phi = 0$: In this case, $J(k_p,k_\tau,k_\theta,k_\phi)$ is the minimum value between $\begin{cases} J((p_i,\tau_i,\phi_i) = (p_j,\tau_j,\phi_j), \theta_i \neq \theta_j), \\ J((p_i,\theta_i,\phi_i) = (p_j,\theta_j,\phi_j), \tau_i \neq \tau_j). \end{cases}$ the optimal $\mathcal{P} = \{1\}$, $\Theta = \{\theta_0 + i\Delta\theta\}_{i=0}^{2^{k_\theta}-1}$, where $\theta_0 = 0$ and $\Delta\theta = \frac{\pi/2}{2^{k_\theta}-1}$; $\Phi = \{1\}$. The optimal $\mathcal{T} = \{0, \Delta\tau, \cdots, \tau_c\}$ with $\Delta\tau = \frac{\tau_c}{2^{k_\tau}-1}$ and $0 \le \tau_c \le \frac{\pi}{4}$ satisfying $\cos(2\tau_c)\sin(\Delta\theta) = \sin\frac{\tau_c}{2^{k_\tau}-1}$. In such a case, we have $d_{R_1}(k_p,k_\tau,k_\theta,k_\phi) = 2\sin(\frac{\Delta\tau}{2})$. This completes the proof of case 13.

(c) $k_\phi \neq 0$, $k_p = 0$, and $k_\theta = 0$: In this case, $J(k_p,k_\tau,k_\theta,k_\phi)$ is the minimum value between $\begin{cases} J((p_i,\tau_i,\theta_i) = (p_j,\tau_j,\theta_j), \phi_i \neq \phi_j), \\ J((p_i,\theta_i,\phi_i) = (p_j,\theta_j,\phi_j), \tau_i \neq \tau_j). \end{cases}$ By the max-min rule, we can attain the optimal $\mathcal{P} = \{1\}$, and $\hat{\Phi} = 2^{k_\phi}$-PSK. We assume $\theta_i = \theta_j = \theta_c$, then we have

$$\Xi(\theta_i,\theta_j,\phi_i,\phi_j) - 1 = -\sin^2(2\theta_c)\sin^2\frac{\pi}{2^{k_\phi}}. \tag{B.18}$$

Then, we obtain the optimal $\Theta = \{\frac{\pi}{4}\}$ and $\mathcal{T} = \{0, \Delta\tau, \cdots, \tau_c\}$ with $\Delta\tau = \frac{\tau_c}{2^{k_\tau}-1}$, and τ_c satisfying

$$\cos(2\tau_c)\sin(\frac{\Delta\phi}{2}) = \sin\frac{\tau_c}{2^{k_\tau}-1}. \tag{B.19}$$

In such a case, we have $d_{R_1}(k_p,k_\tau,k_\theta,k_\phi) = 2\sin(\frac{\Delta\tau}{2})$. This completes the case 14.

3. All of k_p, k_θ, and k_ϕ are zeros, and there exists one scenario: In this case, we have $J(k_p,k_\tau,k_\theta,k_\phi) = J((p_i,\theta_i,\phi_i) = (p_j,\theta_j,\phi_j), \tau_i \neq \tau_j)$. By the max-min rule, we have the optimal $\mathcal{P} = \{1\}$, $\Theta = \{\frac{\pi}{4}\}$, and, $\Phi = \{1\}$. The optimal $\mathcal{T} = \{0, \Delta\tau, \cdots, \frac{\pi}{4}\}$ with $\Delta\tau = \frac{\pi}{4\times(2^{k_\tau}-1)}$. In this case, we have $J(k_p,k_\tau,k_\theta,k_\phi) = 4\sin^2\frac{\pi}{8(2^{k_\tau}-1)}$. In such a case, we have $d_{R_1}(k_p,k_\tau,k_\theta,k_\phi) = 2\sin(\frac{\Delta\tau}{2})$. This completes the case of 15.

This completes the proof of Proposition 2.

References

[1] T. L. Marzetta, "Noncooperative cellular wireless with unlimited numbers of base station antennas," *IEEE Transactions on Wireless Communications*, vol. 9, no. 11, pp. 3590–3600, 2010.

[2] P. Popovski, J. J. Nielsen, C. Stefanovic, E. De Carvalho, E. Strom, K. F. Trillingsgaard, A.-S. Bana, D. M. Kim, R. Kotaba, J. Park, *et al.*, "Wireless access for ultra-reliable low-latency communication: Principles and building blocks," *IEEE Network*, vol. 32, no. 2, pp. 16–23, 2018.

[3] P. Popovski, C. Stefanovic, J. J. Nielsen, E. D. Carvalho, and A. S. Bana, "Wireless access in ultra-reliable low-latency communication (URLLC)," *IEEE Transactions on Communications*, vol. 67, no. 8, pp. 1–1, 2019.

[4] G. Durisi, T. Koch, and P. Popovski, "Toward massive, ultrareliable, and low-latency wireless communication with short packets," *Proceedings of the IEEE*, vol. 104, no. 9, pp. 1711–1726, 2016.

[5] H. Q. Ngo, E. G. Larsson, and T. L. Marzetta, "Energy and spectral efficiency of very large multiuser MIMO systems," *IEEE Transactions on Communications*, vol. 61, no. 4, pp. 1436–1449, 2013.

[6] S. Xue, Y. Ma, and N. Yi, "End-to-end learning for uplink MU-SIMO joint transmitter and non-coherent receiver design in fading channels," *IEEE Transactions on Wireless Communications*, vol. 20, no. 9, pp. 5531–5542, 2021.

[7] R. H. Gohary and H. Yanikomeroglu, "Noncoherent MIMO signaling for block-fading channels: Approaches and challenges," *IEEE Vehicular Technology Magazine*, vol. 14, no. 1, pp. 80–88, 2019.

[8] B. M. Hochwald and W. Sweldens, "Differential unitary space-time modulation," *IEEE Transactions on Communications*, vol. 48, no. 12, pp. 2041–2052, 2000.

[9] B. M. Hochwald, T. L. Marzetta, T. J. Richardson, W. Sweldens, and R. Urbanke, "Systematic design of unitary space-time constellations,"

IEEE Transactions on Information Theory, vol. 46, no. 6, pp. 1962–1973, 2000.

[10] B. M. Hochwald and T. L. Marzetta, "Unitary space-time modulation for multiple-antenna communications in Rayleigh flat fading," *IEEE Transactions on Information Theory*, vol. 46, no. 2, pp. 543–564, 2000.

[11] X.-B. Liang and X.-G. Xia, "Unitary signal constellations for differential space-time modulation with two transmit antennas: parametric codes, optimal designs, and bounds," *IEEE Transactions on Information Theory*, vol. 48, no. 8, pp. 2291–2322, 2002.

[12] G. Li and F.-K. Gong, "Space-time uplink transmission in non-coherent systems with receiver having massive antennas," *IEEE Communications Letters*, vol. 21, no. 4, pp. 929–932, 2016.

[13] S. Li, J.-K. Zhang, and X. Mu, "Noncoherent massive space-time block codes for uplink network communications," *IEEE Transactions on Vehicular Technology*, vol. 67, no. 6, pp. 5013–5027, 2018.

[14] S. Li, J.-K. Zhang, and X. Mu, "Design of optimal noncoherent constellations for SIMO systems," *IEEE Transactions on Communications*, vol. 67, no. 8, pp. 5706–5720, 2019.

[15] A. Manolakos, M. Chowdhury, and A. Goldsmith, "Energy-based modulation for noncoherent massive SIMO systems," *IEEE Transactions on Wireless Communications*, vol. 15, no. 11, pp. 7831–7846, 2016.

[16] H. Xie, W. Xu, W. Xiang, B. Li, and R. Wang, "Performance of ED-based non-coherent massive SIMO systems in correlated Rayleigh fading," *IEEE Access*, vol. 7, pp. 14058–14069, 2019.

[17] H. Xie, W. Xu, H. Q. Ngo, and B. Li, "Non-coherent massive MIMO systems: A constellation design approach," *IEEE Transactions on Wireless Communications*, vol. 19, no. 6, pp. 3812–3825, 2020.

[18] S. Li, X. Guo, H. Lu, S. Huang, and J. Sun, "Cooperative PSK constellation design and power allocation for massive MIMO uplink communications," *Digital Signal Processing*, vol. 111, p. 102935, 2021.

[19] B. Hassibi and B. M. Hochwald, "How much training is needed in multiple-antenna wireless links?," *IEEE Transactions on Information Theory*, vol. 49, no. 4, pp. 951–963, 2003.

[20] V. Erceg, "TGn channel models," *atftp://ieee: wireless@ ftp. 802wirelessworld. com/11/03/11-03-0940-04-000n-tgn-channel-models. doc*, 2004.

[21] K. Kim, J. Lee, and H. Liu, "Spatial-correlation-based antenna grouping for MIMO systems," *IEEE Transactions on Vehicular Technology*, vol. 59, no. 6, pp. 2898–2905, 2010.

[22] P. Pajusco, N. Malhouroux-Gaffet, and G. El Zein, "Comprehensive characterization of the double directional UWB residential indoor channel," *IEEE Transactions on Antennas and Propagation*, vol. 63, no. 3, pp. 1129–1139, 2015.

[23] V. A. Aalo, "Performance of maximal-ratio diversity systems in a correlated Nakagami-fading environment," *IEEE Transactions on Communications*, vol. 43, no. 8, pp. 2360–2369, 1995.

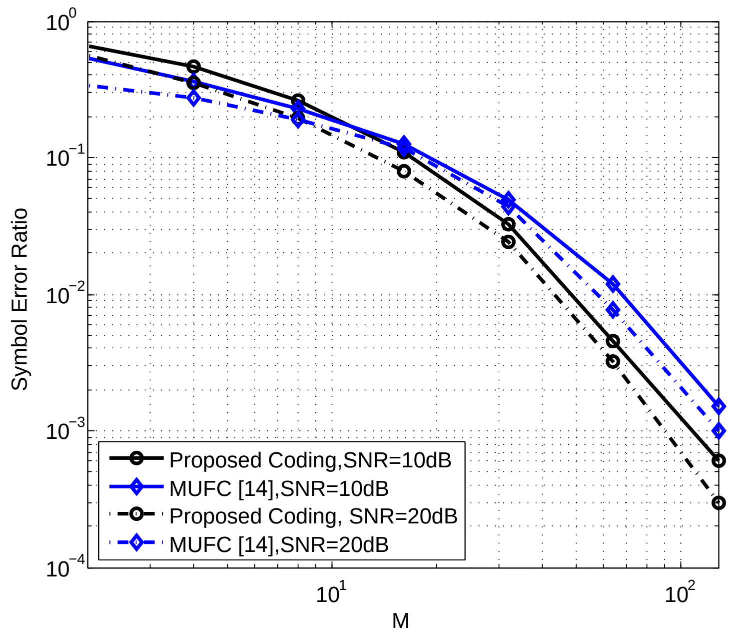

(a)

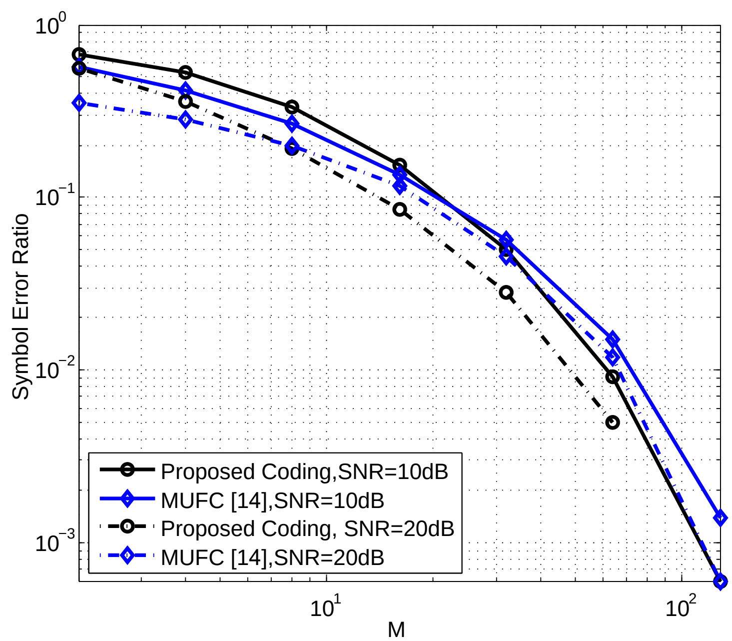

(b)

Figure 2: (a) $\gamma = 0.1$. (b) $\gamma = 0.5$.

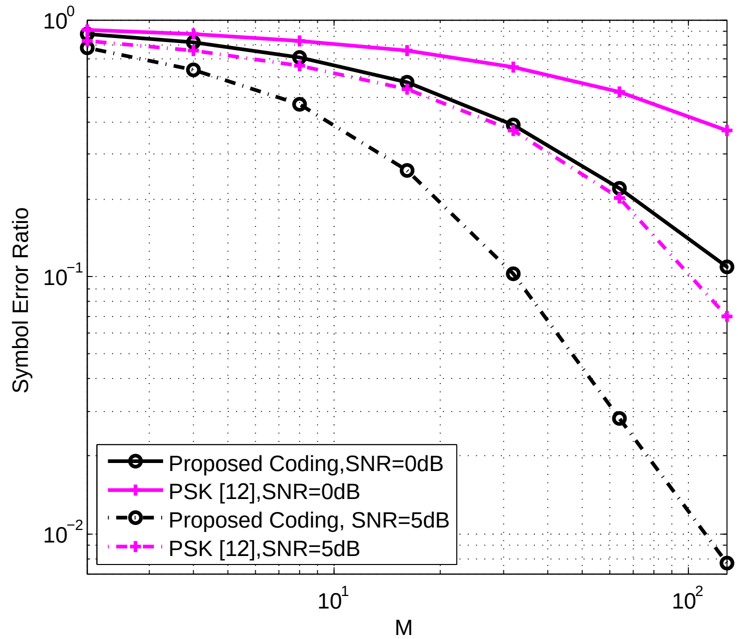

(a)

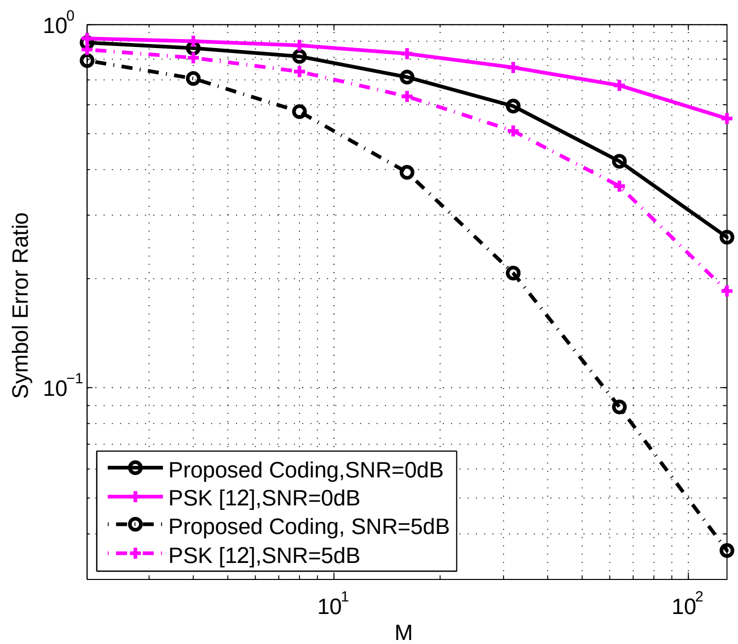

(b)

Figure 3: (a) $\gamma = 0.1$. (b) $\gamma = 0.5$.

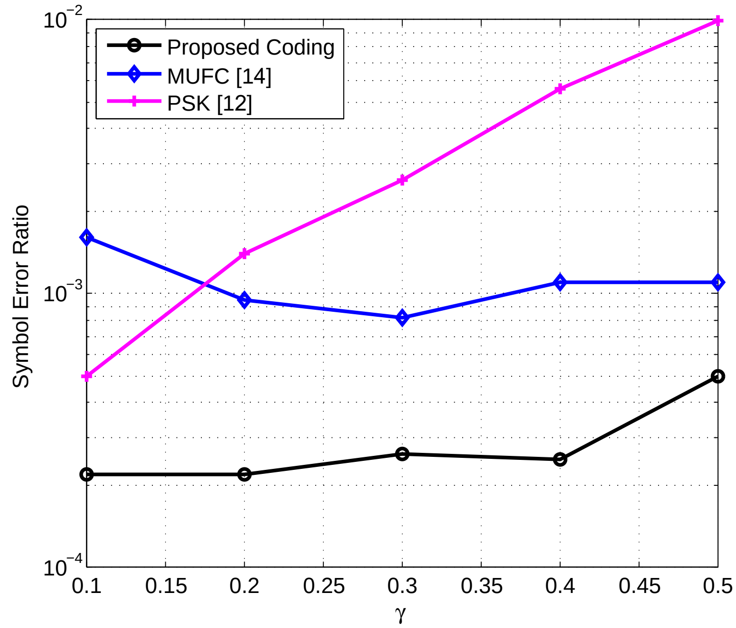

Figure 4: SER vs the correlation coefficient.

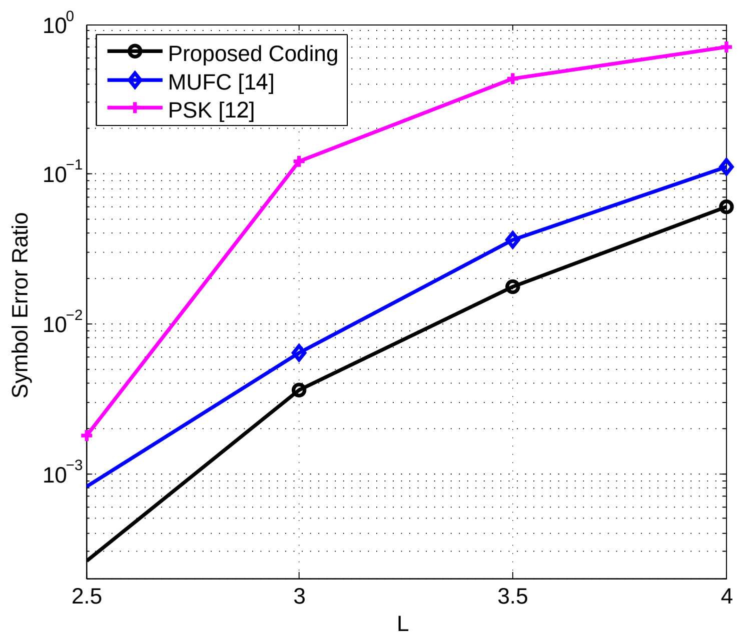

Figure 5: SER vs The transmit rate per channel use.

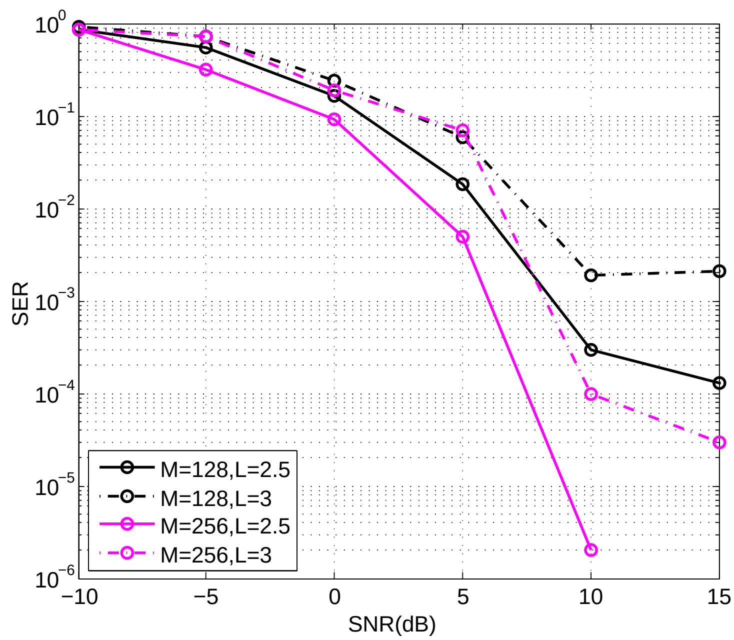

Figure 6: SER vs SNR when $\gamma = 0.3$.